

CLINICAL RESEARCH ARTICLE



Right ventricular function in β -thalassemia children: comparing three-dimensional echocardiography with other functional parameters

Eslam E. Elhawary¹✉, Osama A. Tolba², Asmaa A. Elkaffas¹ and Ahmed H. Shabana²

© The Author(s), under exclusive licence to the International Pediatric Research Foundation, Inc 2021

BACKGROUND: Cardiomyopathy is a major cause of mortality and morbidity in beta-thalassemia major (β -TM), and its early detection is critical for prompt management. We aimed to evaluate right ventricle (RV) function in β -TM, in absence of cardiac symptoms, using 3D echocardiography, and compare it with other functional parameters.

METHODS: Cross-sectional cohort study was conducted on 50 β -TM children with no cardiac manifestations and 50 healthy controls of matched age and sex. We evaluated RV function using; Fraction Area Change (2DE-RV FAC), Ejection Fraction (3D-RVEF), Tricuspid annular plane systolic excursion (TAPSE), Tissue Doppler imaging (TDI) systolic (S') and diastolic (E' , A'), Myocardial performance index (MPI), and speckle tracking (2D-STE) of RV global longitudinal strain (LSS), systolic strain rate (SSR), early diastolic strain rate (DSR E), and late diastolic strain rate (DSR A).

RESULTS: 3D-RVEF, MPI, and 2D-STE showed significant differences between the two groups. ROC curve analysis measurements had an AUC above 0.7—which indicate at least a fair discriminatory power between the β -TM group with RV dysfunction and normal controls.

CONCLUSIONS: β -TM patients have decreased RV function indices at a pre-symptomatic stage. Early detection of RV dysfunction is feasible and can allow for closer follow-up to detect pre-clinical changes.

Pediatric Research (2022) 91:1709–1714; <https://doi.org/10.1038/s41390-021-01900-0>

IMPACT:

- The key message of this article is to emphasize the importance of the evaluation of right ventricular function in children with beta-thalassemia major.
- This article adds to the existing literature the use of recent echocardiographic modalities as three-dimensional echocardiography and two-dimensional speckle tracking in the evaluation of right ventricular dysfunction in beta-thalassemia children while cardiac affection is still subclinical.
- *Impact:* Recent echocardiographic functional parameters can be effectively used to evaluate the right ventricle in beta-thalassemia and can detect dysfunction in asymptomatic patients allowing for early intervention.

INTRODUCTION

Beta-thalassemia major (β -TM) is a public health problem in Egypt, with an estimated incidence of 1000 children/1.5 million live birth per year.¹ The majority of β -TM patients are transfusion-dependent. Lifelong blood transfusions, extravascular hemolysis, and increased gastrointestinal iron lead to iron overload causing tissue and organ damage, especially to the heart.^{2,3}

Chelation therapy can dramatically improve, but not completely eliminate, cardiac involvement and prognosis. Once congestive heart failure develops, a moderate to severe reduction of left ventricular systolic function usually persists, symptoms and signs of severe right-sided heart failure are evident and the prognosis is considered poor. Predominant right heart failure has been attributed to pulmonary hypertension, which was postulated to

occur secondary to lung tissues hemochromatosis or hemochromatosis of the pulmonary vessels.⁴

Cardiomyopathy is a well-known complication of β -TM and the main cause of death in those patients is congestive heart failure.⁵ The process of cardiac affection is gradual, and the cardiac muscle is affected before the appearance of clinical manifestations which makes defining methods of early detection of cardiac dysfunction a crucial step in the routine patient care.³

In a routine echocardiographic evaluation of β -TM patients, most of the examiners focus mainly on the assessment of the left ventricle (LV) function forgetting the right ventricle (RV). Sharing the interventricular septum (IVS), the RV and the LV are functionally linked together. The RV contains transverse muscle fibers in its free wall in addition to sharing oblique fibers in the IVS

¹Hematology and Bone Marrow Transplantation Unit, Pediatrics Department, Faculty of Medicine, Tanta University, Tanta, Egypt. ²Cardiology Unit, Pediatrics Department, Faculty of Medicine, Tanta University, Tanta, Egypt. ✉email: eslam.elhawary@med.tanta.edu.eg

Received: 4 March 2021 Revised: 4 October 2021 Accepted: 12 October 2021

Published online: 14 December 2021

with the LV, thus LV contraction contributes to the RV contraction via the IVS, which is why assessment of RV function in those patients is of vital importance.⁶

RV function can be evaluated by a variety of echocardiographic quantitative measures. Two-dimensional Functional Area Change (2D-RV FAC) provides an estimate of RV systolic function. Tricuspid annular plane systolic excursion (TAPSE) is an M-mode parameter that reflects longitudinal shortening of the RV.⁷ Tissue Doppler imaging (TDI) is used for measurement of the peak myocardial velocity and time, but this modality could be affected by the angle of ultrasound beams to the targeted myocardial wall in addition to being load-dependent.⁸

Two-dimensional speckle tracking echocardiography (2D-STE) is a relatively novel imaging modality providing quantitative evaluation of global and regional myocardial deformation independent from the ultrasound beam angle and cardiac translational movements, overcoming TDI limitations.^{9,10}

Evaluation of RV function, volume, and mass are considered challenging owing to its unique cavity geometry. Although evaluation of the RV focused on the use of 2-dimensional echocardiography (2DE), progressive development of three-dimensional echocardiography (3DE) made it possible to evaluate the RV with more accuracy.¹¹

It is reasonable to assume that 3DE measurement of volumes and ejection fraction might improve assessment of RV function, that's why we aimed in this study to evaluate the RV function in β -TM children using 3DE and to compare these parameters with conventional echo, TDI, and speckling tracking derived parameters.

PATIENTS AND METHODS

This cross-sectional cohort study was conducted on 50 children diagnosed with β -TM with no clinically evident cardiac manifestations. All the patients received packed red blood cell transfusions every 3-4 weeks to sustain a hemoglobin level above 8 g/dl. All the enrolled patients had serum ferritin level exceeding 1000 ng/ml and received iron chelation in the form of deferasirox (EXJADE 30 mg/kg/day or JADENU 20 mg/kg/day). They were selected from those attending the outpatient clinic before regular transfusion at The Hematology Unit, Pediatrics Department of Tanta University Hospital. Fifty healthy children served as a control group with matched age and sex, they were recruited from healthy children attending the outpatient clinic for routine well child visits. Informed written consent was obtained from the guardians of enrolled children. The study was approved by the ethical committee of the Faculty of Medicine, Tanta University.

Full history taking, general and regional examinations were performed and children with congenital or other acquired heart diseases were excluded. The laboratory investigations included serum ferritin and a complete blood count prior to transfusion.

Echocardiographic images were obtained using a Vivid 7 ultrasound machine (GE Medical System, Horten, Norway). Data acquisition was done using a 3.5-MHz transducer, S7, and V3 matrix real-time 3-dimensional probes. We used the following quantitative echocardiographic parameters to measure RV function:

2D-RV FAC is the percent change in RV area from diastole to systole, a 2D substitute for ejection fraction, and it reflects the systolic function of the inflow as well as the apical portions of the RV. FAC represents longitudinal shortening as well as a radial thickening in addition to the contribution of the interventricular septum.⁷ 2D-RV FAC was measured using transthoracic 2DE examination in the apical 4-chamber view by manually tracing the RV contour at end-diastole and end-systole. The 2D-RV FAC was calculated as follows:

$$\text{FAC} = \frac{[(\text{end-diastolic RV area} - \text{end-systolic RV area}) / \text{end-diastolic RV area}] \times 100}{}$$

TAPSE was measured in the apical 4-chamber view by placing an M-mode cursor on the lateral tricuspid annulus and measuring the peak distance traveled by this reference point during systole. TAPSE is a reflection of longitudinal shortening of the RV.¹²

TDI was done with a sample volume of 5.5 mm, a frame rate of greater than 150 fps and the average velocities of 3 consecutive cycles were recorded to reduce the effect of respiration on blood velocities and as breath-holding is not applicable in young children. Systolic (S') and diastolic (E', A') myocardial velocities were measured in the apical 4-chamber view by placing a tissue Doppler cursor on the lateral tricuspid annulus and measuring the peak velocity of this reference point during systole and diastole. S' reflects the longitudinal velocity of the tricuspid annulus during systole, and the greater the velocity during systole the greater the RV systolic function.¹³

Myocardial performance index (MPI, Tei index): was measured using this formula: $(a - b)/b$, where "a" is the time between the end of A wave of tricuspid inflow to the beginning of E wave of tricuspid inflow in the next cardiac cycle obtained by TDI at tricuspid inflow at the apical 4-chamber view, and "b" is the pulmonary ejection time obtained by TDI at the pulmonary valve in parasternal short-axis view. MPI is based on time intervals and is independent of the geometry of cardiac chambers and contraction pattern.¹⁴

2D-STE: Strain is considered as the percent change in the myocardial deformation (predominantly the longitudinal shortening in case of the RV), while strain rate can be defined as the rate of myocardial deformation.¹⁵ 2DE images were obtained using the 3 standard apical views; apical long axis, apical, 4-chamber, and 2-chamber views, and parameters obtained represented the average of 3 cardiac cycles, with a frame rate of 65 fps, and all segmental data were represented. We used automated function imaging that enables the assessment of longitudinal strain available in Vivid 7 ultrasound machine to measure average RV free wall peak global longitudinal strain (LSS), RV free wall global peak systolic strain rate (SSR), RV free wall global early diastolic strain rate (DSR E), and RV free wall peak global late diastolic strain rate (DSR A). The digital loops were stored on a hard disk of the echocardiography machine then transferred for offline analysis to a workstation (Echo PAC PC, 113; GE, Horten, Norway). Acceptable images from three cardiac cycles were digitally saved for offline speckle-tracking analysis. Tracking was accepted not only if the Echo PAC software showed adequate tracking, but also if the examiner's inspection revealed good tracking throughout the cardiac cycle. Automated software tracking is not always reliable, in which case, manual selection of precise landmarks, segmental contouring, and/or a region of interest was paramount to allow optimal manual adjustments.

3-Dimensional Right Ventricular Ejection Fraction (3D-RVEF): 3D images of the RV were obtained in a full-volume data set from the apical 4-chamber view and optimized for analysis of RV function.¹⁶ Multi-beat (3-6 beats) data were obtained on the multislice (short-axis) visualization mode, to make sure that the right ventricle was entirely included in the data set. All the measurements of RV volumes and EF were made offline, using dedicated software (Echo PAC PC, 113; GE, Horten, Norway). Semi-automatic analysis was performed, with a manual tracing of the endocardial borders in end-systolic and end-diastolic frames in the sagittal, 4-chamber, and coronal views, obtained from the full-volume data set. In addition, end-diastolic volume (EDV), end-systolic volume (ESV), stroke volume (SV), and ejection fraction (EF) were calculated using the software (Fig. 1).

Inter- and intra-observer variability analysis: Two echocardiographers independently performed 10 randomized Speckle Tracking analyses for five patients and five controls to analyze inter-observer variability. One observer measured the Speckle Tracking analysis twice in the 10 randomized subjects on two consecutive days for intra-observer variability analysis.

Statistical analysis

Statistical analysis was performed using MedCalc Statistical Software version 15.8 (MedCalc Software bvba, Ostend, Belgium; <https://www.medcalc.org>; 2015). The distribution of numerical variables was determined according to the Shapiro Wilk test as well as the shape of the distribution in histograms and Q-Q plots. Variables that followed normal distribution were summarized as mean \pm standard deviation (SD) and range (minimum and maximum values). Comparisons between the two groups were performed using independent samples *t*-test. For variables that did not follow a normal distribution, median, interquartile range (IQR, expressed as 25th percentile–75th percentile), and range (minimum, maximum) were calculated. Mann–Whitney *U* test was used to compare the two groups. Receiver operating characteristic (ROC) curve analysis was performed to analyze the relation between true-positive and false-positive results for each measured parameter and to identify the best cut-off value that yields

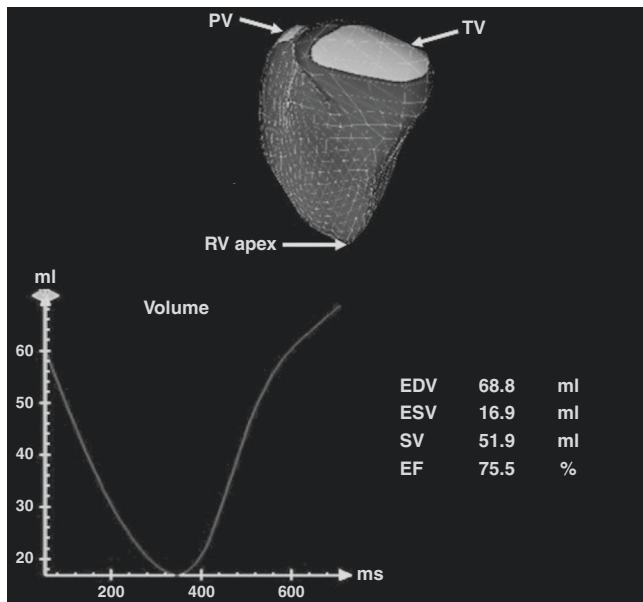


Fig. 1 Example of a three-dimensional echocardiographic reconstruction of the delineation of the right ventricle seen from the septal side. The mesh in gray is the right ventricle at end-diastole. The curve represents right ventricular volume end-systole. The pulmonary valve (PV) is shown in white in the upper left side, tricuspid valve (TV) is shown in the upper right side, and right ventricular (RV) apex toward the bottom. EDV The end-diastolic volume = 68.8 ml, ESV: end-systolic volume = 16.9 ml, SV stroke volume = 51.9 ml, and EF ejection fraction = 75.5%.

both the highest sensitivity and specificity. The discriminatory power of AUC was graded as follows: 0.90–1 = excellent; 0.80–0.90 = good; 0.70–0.80 = fair; and 0.60–0.70 = poor. Pairwise comparisons were performed between the AUCs of the studied parameters according to the method described by DeLong et al.¹⁷ The significance of tests was adopted at a P -value < 0.05.

RESULTS

The mean age of children in the β -TM group was 8.57 ± 4.75 years and that of the control group was 7.96 ± 3.97 years. The β -TM group included 27 females and 23 males while the control group included 24 females and 26 males. Family history of thalassemia was positive in 43 patients and 35 patients were products of consanguineous marriage. The body mass index of patients was 18.73 ± 5.32 kg/m² which was comparable to that of the control group (17.68 ± 4.89 kg/m²). The mean hemoglobin level in the patients' group was 7.23 ± 1.35 gm/dl, which was significantly lower than the control group (11.80 ± 1.74 gm/dl) and the serum ferritin median level was 1850 ng/ml (range: 1259–8753 ng/ml) in patients' group, which was significantly higher than the control group (83.52 ± 11.37 ng/ml).

3D evaluation of the RVEF revealed a significant increase when compared with the control group (P -value < 0.001). TDI-derived MPI also showed a statistically significant increase in patients compared to the control group. The 2D-STE of right ventricular strain (LSS) and strain rates (SSR, DSR E, and DSR A) were significantly decreased in patients than in controls. There was no significant difference between the two groups as regard TAPSE, 2D-RV FAC, tricuspid annulus systolic tissue Doppler velocity (S'), tricuspid annulus early diastolic velocity (E'), or tricuspid annulus late tissue Doppler velocity (A') (Table 1).

As we can see in Table 2 and Fig. 2, the results of ROC curve analysis for the diagnosis of RV dysfunction using the studied measurements. All measurements had an AUC above 0.7—which indicate at least a fair discriminatory power between β -TM group

with RV dysfunction and those without (normal controls). TDI-derived RV MPI had the highest AUC (AUC = 0.982, 95% CI = 0.909–0.999), followed by 3DE-RVEF (AUC = 0.974, 95% CI = 0.896–0.998), then 2D-STE SSR (AUC = 0.804, 95% CI = 0.681–0.895), 2D-STE DSR A (AUC = 0.762, 95% CI = 0.635–0.863), 2D-STE LSS (AUC = 0.748, 95% CI = 0.619–0.851), and 2D-STE DSR E (AUC = 0.739, 95% CI = 0.610–0.844). The AUCs of TDI-derived MPI and 3DE-RVEF did not differ significantly (P -value = 0.675), but both were significantly higher than the AUCs of the other measurements (P -value < 0.05). There was no statistically significant difference among the AUCs of Speckle tracking LSS, SSR, DSR E, and DSR A (P -value > 0.05). The best cut-off values for each measurement and its associated sensitivity and specificity are demonstrated in Table 2.

DISCUSSION

Cardiomyopathy is the primary determinant of prognosis and survival in β -TM.¹⁸ Its early detection is markedly needed. In our study, we focused on the detection of RV dysfunction in the pre-symptomatic stage using echocardiography as a diagnostic tool. We used a variety of modalities including 3DE, conventional echo, TDI, and 2D-STE strain analysis focusing on RV evaluation.

Assessment of RV size and function should be part of every echocardiographic examination at the time of diagnosis and during regular follow-up in β -TM. Guidelines for the echocardiographic evaluation of the RV emphasize the importance of combining different echocardiographic parameters for obtaining full coverage of the different RV structural and functional assessment.¹⁹

In the current study, we were able to detect a significant difference between patients and controls as regard TDI-derived RV MPI, with a mean of 0.63 ± 0.15 and 0.35 ± 0.08 , respectively, and P -value < 0.001. Lower values indicate better function since the healthy RV should theoretically spend a shorter time in the isovolumetric phase and a greater proportion ejecting blood. Since MPI is usually affected before other RV parameters, it can be a more sensitive parameter for subclinical or early RV dysfunction detection.⁷

Tricuspid annulus systolic tissue Doppler velocity (S'), tricuspid annulus early diastolic velocity (E'), and tricuspid annulus late tissue Doppler velocity (A') showed no significant difference between the two groups. TDI has the limitations of being angle-dependent and load-dependent, and the determination of tissue velocity is influenced by the global cardiac translation as well as tricuspid regurgitation.¹⁷

Conventional 2D-RV FAC revealed no statistically significant difference between patients and controls with a mean of $41.57 \pm 7.68\%$ and $39.33 \pm 1.88\%$, respectively. Assessment of RV volumes using 2D echocardiography can be challenging. 2D-RV measurements show poor agreement with more advanced and accurate imaging modalities as 3D volumes calculated by cardiac magnetic resonance (CMR).^{20,21} This definitely underestimates the true RV volumes as the RV outflow tract is not included in the conventional 2D assessment.²²

We also found that TAPSE showed no significant difference between the β -TM group and the control group with a mean of 19.23 ± 3.56 and 20.17 ± 1.86 mm, respectively. The major limitation of TAPSE is that it can only represent one component of RV motion within one single segment of RV myocardium. The RV may be clearly dysfunctional yet preserving relatively normal TAPSE. Also, TAPSE measures displacement relative to the stationary transducer, which may produce misleading results.²³

The use of 3D estimation of the RVEF showed higher values in patients than in controls ($62.97 \pm 6.47\%$ and $49.50 \pm 4.18\%$, respectively) with a P -value < 0.001. Both 3D echocardiography and CMR seem to offer better discrimination, in particular using RV ejection fraction impairment in addition to absolute volume cut-

Table 1. Right ventricular parameters of the studied groups.

	β-TM (n = 50)	Control (n = 50)	Statistical test	P-value
2DE-RV FAC (%) ^a	41.57 ± 7.68	39.33 ± 1.88	1.547 ^c	0.132
3DE-RV EF (%) ^a	62.97 ± 6.47	49.50 ± 4.18	9.576 ^c	<0.001*
TAPSE (mm) ^a	19.23 ± 3.56	20.17 ± 1.86	1.273 ^c	0.210
RV MPI by TDI ^a	0.63 ± 0.15	0.35 ± 0.08	9.151 ^c	<0.001*
S' velocity RV (cm/s) ^a	6.73 ± 1.01	6.97 ± 0.85	2.217 ^c	0.231
E' velocity RV (cm/s) ^a	11.83 ± 2.15	12.67 ± 1.21	1.848 ^c	0.071
A' velocity RV (cm/s) ^a	6.23 ± 1.43	6.47 ± 1.20	0.685 ^c	0.496
2D-STE LSS (%) ^b	18.00 (15.00–21.00)	−23.00 (−25.00–20.00)	3.303 ^d	0.001*
2D-STE SSR (%) ^b	1.10 (0.89–1.40)	1.50 (1.50–1.90)	4.059 ^d	<0.001*
2D-STE DSR E (1/S) ^a	1.57 ± 0.64	2.15 ± 0.55	3.746 ^c	<0.001*
2D-STE DSR A (1/S) ^a	0.73 ± 0.35	1.04 ± 0.25	3.961 ^c	<0.001*

β-TM beta-thalassemia major, 2DE-RV FAC 2-Dimensional Right Ventricular Fraction Area Change, 3DE-RV EF 3-Dimensional Right Ventricular Ejection Fraction, TAPSE Tricuspid annular plane systolic excursion, RV MPI Right ventricular myocardial performance index, TDI tissue Doppler imaging, S' Tricuspid annulus systolic tissue Doppler velocity, E' Tricuspid annulus early diastolic velocity, A' Tricuspid annulus late tissue Doppler velocity, 2D-STE 2-dimensional speckle tracking echocardiography, LSS right ventricle-free wall peak global longitudinal strain, SSR right ventricle-free wall global peak systolic strain rate, DSR E right ventricle-free wall peak global early diastolic strain rate, DSR A right ventricle-free wall peak global late diastolic strain rate.

*Significant at P-value < 0.05.

^aData are expressed as mean ± SD (standard deviation).

^bData are expressed as median and IQR: interquartile range (25th–75th percentiles).

^cIndependent samples t-test.

^dMann–Whitney test.

Table 2. ROC curve analysis of right ventricular parameters.

Parameters	AUC (95% CI)	P-value (against AUC = 0.5)	Cut-off value	Sensitivity (%)	Specificity (%)
RV MPI by TDI	0.982 (0.909–0.999)	<0.001*	>0.4	96.67	93.33
3DE-RVEF (%)	0.974 (0.896–0.998)	<0.001*	>55	90.00	96.67
2D-STE LSS (%)	0.748 (0.619–0.851)	<0.001*	>−22	100.0	66.67
2D-STE SSR (%)	0.804 (0.681–0.895)	<0.001*	≤1.4	76.67	76.67
2D-STE DSR E (1/S)	0.739 (0.610–0.844)	<0.001*	≤1.3	46.67	96.67
2D-STE DSR A (1/S)	0.762 (0.635–0.863)	<0.001*	≤0.7	53.33	96.67
P-value from pairwise comparisons of AUCs	RV MPI by TDI vs 3DE-RVEF = 0.675				
	RV MPI by TDI vs 2D-STE LSS = 0.001*				
	RV MPI by TDI vs 2D-STE SSR = 0.003*				
	RV MPI by TDI vs 2D-STE DSR E < 0.001*				
	RV MPI by TDI vs 2D-STE DSR A = 0.001*				
	3DE-RVEF vs 2D-STE LSS < 0.001*				
	3DE-RVEF vs 2D-STE SSR = 0.006*				
	3DE-RVEF vs 2D-STE DSR E < 0.001*				
	3DE-RVEF vs 2D-STE DSR A = 0.002*				
	2D-STE LSS vs 2D-STE SSR = 0.569				
	2D-STE LSS vs 2D-STE DSR E = 0.933				
	2D-STE LSS vs 2D-STE DSR A = 0.884				
	2D-STE SSR vs 2D-STE DSR E = 0.311				
2D-STE SSR vs 2D-STE DSR A = 0.625					
2D-STE DSR E vs 2D-STE DSR A = 0.823					

RV MPI Right ventricular myocardial performance index, TDI tissue Doppler imaging, 3DE-RV EF 3-Dimensional Right Ventricular Ejection Fraction, 2D-STE 2-Dimensional speckle tracking echocardiography, LSS right ventricle-free wall peak global longitudinal strain, SSR right ventricle-free wall global peak systolic strain rate, DSR E right ventricle-free wall peak global early diastolic strain rate, DSR A right ventricle-free wall peak global late diastolic strain rate.

ROC receiver operating characteristic, AUC area under the ROC curve, CI confidence interval.

*Significant at P-value < 0.05.

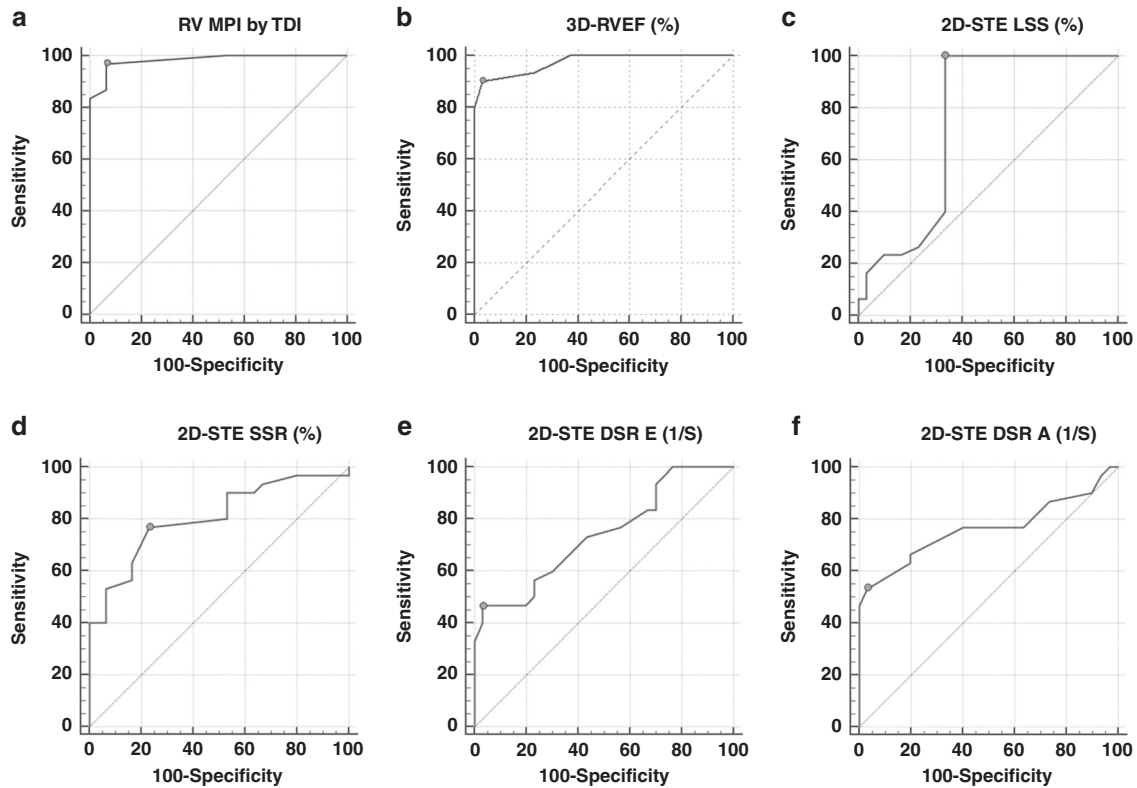


Fig. 2 ROC curve analysis of right ventricular function using different echocardiographic parameters. The circle indicates the optimal cut-off value. The diagonal line represents the null hypothesis AUC of 0.5. **a** ROC curve analysis of right ventricular myocardial performance index (MPI) derived from tissue Doppler imaging (TDI). (AUC = 0.982, 95% CI = 0.909–0.999, Cut-off value > 0.4, Sensitivity = 96.67%, Specificity = 93.33%, **P*-value < 0.001). **b** ROC curve analysis of 2-dimensional right ventricular ejection fraction (3D-RVEF). (AUC = 0.974, 95% CI = 0.896–0.998, Cut-off value > 55, Sensitivity = 90%, Specificity = 96.96%, **P*-value < 0.001). **c** ROC curve analysis of right ventricle-free wall peak global longitudinal strain (LSS) measured by 2-dimensional speckle tracking echocardiography (2D-STE). (AUC = 0.748, 95% CI = 0.619–0.851, Cut-off value > –22, Sensitivity = 100%, Specificity = 66.67%, **P*-value < 0.001). **d** ROC curve analysis of right ventricle-free wall global peak systolic strain rate (SSR) measured by 2-dimensional speckle tracking echocardiography (2D-STE). (AUC = 0.804, 95% CI = 0.681–0.895, Cut-off value ≤ 1.4, Sensitivity = 76.67%, Specificity = 76.67%, **P*-value < 0.001). **e** ROC curve analysis of right ventricle-free wall global peak early diastolic strain rate (DSR E) measured by 2-dimensional speckle tracking echocardiography (2D-STE). (AUC = 0.739, 95% CI = 0.610–0.844, Cut-off value ≤ 1.3, Sensitivity = 46.67%, Specificity = 96.67%, **P*-value < 0.001). **f** ROC curve analysis of right ventricle-free wall global peak late diastolic strain rate (DSR A) measured by 2-dimensional speckle tracking echocardiography (2D-STE). (AUC = 0.762, 95% CI = 0.635–0.863, Cut-off value ≤ 0.7, Sensitivity = 53.33%, Specificity = 96.67%, **P*-value < 0.001).

offs.²⁴ Overall, there is a good to reasonable correlation between RV volumes and ejection fraction measured by CMR and 3D echocardiography.²⁵

The challenge of obtaining a high-quality full volumetric 3D data set, including the RV anterior wall and the RV apical lateral segments, in patients with poor imaging windows and/or dilated RV is the main limitation of this method. Moreover, accuracy tends to decrease with increasing RV dilatation, limiting its application in patients with dilated ventricles.^{26,27} The higher RVEF could be caused by the hyperdynamic circulation characteristic of those patients. This denotes that RVEF is load-dependent. So, it's not reasonable to depend solely on this parameter for the detection of early RV systolic dysfunction.

Due to the limitations discussed above regarding the use of 2D-RV FAC, 3D-RV EF, TAPSE, MPI, and TDI assessment of RV remains challenging in clinical practice and is often limited to subjective qualitative assessment. Recent guidelines recommend performing quantitative measurements of RV function using more than one modality to get reliable results.⁷

The introduction of speckle-tracking echocardiography made the measurement of strain and strain rate easier and is now a well-established modality for the evaluation of the LV. Yet its use to evaluate RV function is limited by lack of reference values. In the current study, the 2D-STE of right ventricular strain and strain rates demonstrated a statistically significant difference (*P*-value < 0.001)

as regard LSS, SSR, DSR E, and DSR A. These denote silent systolic and diastolic dysfunction in those children. Speckle tracking-based assessment of global LV function has received much recent attention. It was found more sensitive in detecting early functional impairment than volume-based functional indices such as ejection fraction in several clinical scenarios.²⁸

ROC curve analysis for the diagnosis of RV dysfunction revealed that all measurements had an AUC above 0.7—which indicate at least a fair discriminatory power between β -TM group with RV dysfunction and those without (normal controls). TDI-derived RV MPI had the highest AUC (AUC = 0.982, 95% CI = 0.909–0.999), followed by 3DE-RVEF (AUC = 0.974, 95% CI = 0.896–0.998), then 2D-STE SSR (AUC = 0.804, 95% CI = 0.681–0.895), 2D-STE DSR A (AUC = 0.762, 95% CI = 0.635–0.863), 4D-STE LSS (AUC = 0.748, 95% CI = 0.619–0.851), and 2D-STE DSR E (AUC = 0.739, 95% CI = 0.610–0.844). The AUCs of TDI-derived MPI and 3DE-RVEF did not differ significantly (*P*-value = 0.675), but both were significantly higher than the AUCs of the other measurements (*P*-value < 0.05). There was no statistically significant difference among the AUCs of Speckle tracking LSS, SSR, DSR E, and DSR A (*P*-value > 0.05).

Although developed for the LV, speckle tracking has been applied to the RV.²⁹ Peak longitudinal strain and strain rate measurement are independent of global cardiac motion and allow quantifying regional myocardial deformation in the different RV segments.^{30,31}

CONCLUSION

Children with β -TM have decreased RV function indices at a pre-symptomatic stage. Early detection of RV dysfunction is feasible by Right ventricular myocardial performance index (RV MPI) using tissue Doppler imaging (TDI), 3-Dimensional Right Ventricular Ejection Fraction (3DE-RV EF), and 2-Dimensional speckle tracking echocardiography (2D-STE), as and can allow for closer follow-up to detect pre-clinical changes. That would be of great value when tailoring individual management plans for patients with β -TM including dosing of iron chelators, frequencies of transfusion, use of cardioprotective agents, and further evaluation using CMR, in order to consequently improve patient survival.

REFERENCES

1. El-Shanshory, M. et al. Spectrum of beta globin gene mutations in Egyptian children with β -thalassemia. *Mediterr. J. Hematol. Infect. Dis.* **6**, e2014071 (2014).
2. Porter, J. B. & Shah, F. T. Iron overload in thalassemia and related conditions: therapeutic goals and assessment of response to chelation therapies. *Hematol. Oncol. Clin. North Am.* **24**, 1109–1130 (2010).
3. Auger, D. & Pennell, D. J. Cardiac complications in thalassemia major. *Ann. N. Y. Acad. Sci.* **1368**, 56–64 (2016).
4. Hahalis, G. et al. Right ventricular cardiomyopathy in β -thalassaemia major. *Eur. Heart J.* **23**, 147–156 (2002).
5. Dhanya, R. et al. Life expectancy and risk factors for early death in patients with severe thalassemia syndromes in South India. *Blood Adv.* **4**, 1448–1457 (2020).
6. Schwarz, K., Singh, S., Dawson, D. & Frenneaux, M. P. Right ventricular function in left ventricular disease: Pathophysiology and implications. *Heart Lung Circul.* **22**, 507–511 (2013).
7. Rudski, L. G. et al. Guidelines for the echocardiographic assessment of the right heart in adults: a report from the American Society of Echocardiography endorsed by the European Association of Echocardiography, a registered branch of the European Society of Cardiology, and. *J. Am. Soc. Echocardiogr.* **23**, 685–688 (2010).
8. Kukulski, T. et al. Normal regional right ventricular function and its change with age: A Doppler Myocardial Imaging study. *J. Am. Soc. Echocardiogr.* **13**, 194–204 (2000).
9. Arbeille, P. et al. Four-dimensional speckle tracking for assessing improvement in left ventricular contractility after coronary angioplasty. *Ultrasound Med. Biol.* **39**, 102–110 (2013).
10. Al-Biltagi, M., Abd Rab Elrasoul Tolba, O., El-Shanshory, M. R., Abd El-Aziz El-Shitany, N. & El-Sayed El-Hawary, E. Strain echocardiography in early detection of doxorubicin-induced left ventricular dysfunction in children with acute lymphoblastic leukemia. *ISRN Pediatr.* **2012**, 1–9 (2012).
11. Shiota, T. 3D echocardiography: evaluation of the right ventricle. *Curr. Opin. Cardiol.* **24**, 410–414 (2009).
12. Lang, R. M. et al. Recommendations for cardiac chamber quantification by echocardiography in adults: an update from the American Society of Echocardiography and the European Association of Cardiovascular Imaging. *J. Am. Soc. Echocardiogr.* **28**, 1–39.e14 (2015).
13. Sade, L. E. et al. Tissue Doppler study of the right ventricle with a multisegmental approach: comparison with cardiac magnetic resonance imaging. *J. Am. Soc. Echocardiogr.* **22**, 361–368 (2009).
14. Kjaergaard, J., Snyder, E. M., Hassager, C., Oh, J. K. & Johnson, B. D. Impact of preload and afterload on global and regional right ventricular function and pressure: a quantitative echocardiography study. *J. Am. Soc. Echocardiogr.* **19**, 515–521 (2006).
15. López-Candales, A. et al. Abnormal right ventricular myocardial strain generation in mild pulmonary hypertension. *Echocardiography* **24**, 615–622 (2007).
16. Maffessanti, F. et al. Age-, body size-, and sex-specific reference values for right ventricular volumes and ejection fraction by three-dimensional echocardiography: a multicenter echocardiographic study in 507 healthy volunteers. *Circ. Cardiovasc. Imaging* **6**, 700–710 (2013).
17. DeLong, E. R., DeLong, D. M. & Clarke-Pearson, D. L. Comparing the areas under two or more correlated receiver operating characteristic curves: a nonparametric approach. *Biometrics* **44**, 837 (1988).
18. Kremastinos, D. T. et al. Special report-thalassemia cardiomyopathy history, present considerations, and future perspectives. *Circ. Heart Fail.* **3**, 451–458 (2010).
19. Lopez, L. et al. Recommendations for quantification methods during the performance of a pediatric echocardiogram: a report from the Pediatric Measurements Writing Group of the American Society of Echocardiography Pediatric and Congenital Heart Disease Council. *J. Am. Soc. Echocardiogr.* **23**, 465–467 (2010).
20. Lai, W. W. et al. Accuracy of guideline recommendations for two-dimensional quantification of the right ventricle by echocardiography. *Int. J. Cardiovasc. Imaging* **24**, 691–698 (2008).
21. Couto, M. et al. Accuracy of right ventricular volume and function assessed with cardiovascular magnetic resonance: comparison with echocardiographic parameters. *Clin. Imaging* **59**, 61–67 (2020).
22. Silverman, N. H. & Hudson, S. Evaluation of right ventricular volume and ejection fraction in children by two-dimensional echocardiography. *Pediatr. Cardiol.* **4**, 197–203 (1983).
23. Giusca, S. et al. Deformation imaging describes right ventricular function better than longitudinal displacement of the tricuspid ring. *Heart* **96**, 281–288 (2010).
24. Vermes, E. et al. Impact of the revision of arrhythmogenic right ventricular cardiomyopathy/dysplasia task force criteria on its prevalence by CMR criteria. *Jacc. Cardiovasc. Imaging* **4**, 282–287 (2011).
25. Shimada, Y. J., Shiota, M., Siegel, R. J. & Shiota, T. Accuracy of right ventricular volumes and function determined by three-dimensional echocardiography in comparison with magnetic resonance imaging: a meta-analysis study. *J. Am. Soc. Echocardiogr.* **23**, 943–953 (2010).
26. Grewal, J., Majdalany, D., Syed, I., Pellikka, P. & Warnes, C. A. Three-dimensional echocardiographic assessment of right ventricular volume and function in adult patients with congenital heart disease: comparison with magnetic resonance imaging. *J. Am. Soc. Echocardiogr.* **23**, 127–133 (2010).
27. Khoo, N. S. et al. Assessments of right ventricular volume and function using three-dimensional echocardiography in older children and adults with congenital heart disease: comparison with cardiac magnetic resonance imaging. *J. Am. Soc. Echocardiogr.* **22**, 1279–1288 (2009).
28. Ostenfeld, E. & Flachs-kampf, F. A. Assessment of right ventricular volumes and ejection fraction by echocardiography: from geometric approximations to realistic shapes. *Echo Res. Pract.* **2**, R1–R11 (2015).
29. Tolba, O. A. R. E., El-Shanshory, M. R., El-Gamasy, M. A. E. & El-Shehaby, W. A. Speckle tracking evaluation of right ventricular functions in children with sickle cell disease. *Ann. Pediatr. Cardiol.* **10**, 230–233 (2017).
30. Dragulescu, A. & Mertens, L. L. Developments in echocardiographic techniques for the evaluation of ventricular function in children. *Arch. Cardiovasc. Dis.* **103**, 603–614 (2010).
31. Mertens, L. L. & Friedberg, M. K. Imaging the right ventricle—current state of the art. *Nat. Rev. Cardiol.* **7**, 551–563 (2010).

AUTHOR CONTRIBUTIONS

O.A.T. provided the research idea and initiated the study design and E.E.E. and A.A.E. helped with implementation. O.A.T. and A.H.S. were responsible for the technical part of the study. All authors substantially contributed to the acquisition, analysis, and interpretation of data for the manuscript and drafting, revising, and critically reviewing the manuscript for important intellectual content. All authors approved the final version of this manuscript to be published and agree to be accountable for all aspects of the work in ensuring that questions related to the accuracy or integrity of any part of the work are appropriately investigated and resolved.

COMPETING INTERESTS

The authors declare no competing interests.

CONSENT STATEMENT

Informed written consent was obtained from the guardian of every child enrolled in the study (both patients and controls).

ADDITIONAL INFORMATION

Correspondence and requests for materials should be addressed to Eslam E. Elhawary.

Reprints and permission information is available at <http://www.nature.com/reprints>

Publisher's note Springer Nature remains neutral with regard to jurisdictional claims in published maps and institutional affiliations.